Adsorption (2007) 13: 341–349
DOI 10.1007/s10450-007-9032-6

A complete experimental approach for synthesis gas separation studies using static gravimetric and column breakthrough experiments

Youssef Belmabkhout · Gerhard Pirngruber · Elsa Jolimaitre · Alain Methivier

Received: 1 May 2007 / Revised: 19 July 2007 / Accepted: 23 July 2007 / Published online: 20 September 2007

Abstract In this work a combination of static gravimetric and inverse chromatographic techniques is used to study the adsorption and separation of the main synthesis gas components, i.e. CO_2, CO, CH_4 and H_2. The single component adsorption isotherms of CO_2, CO, CH_4 and H_2 on faujasite NaX were measured from 303 K to 473 K and over a large range of pressures (from 0 to 1200 kPa). Breakthrough curves of CO_2 and CO and their mixtures were determined at 323 K and 373 K and 100 kPa as an illustrative example. A nice agreement was noticed between the two abovementioned techniques for single component adsorption. Binary mixture dynamics measurements were compared to the predictions of ideal adsorption solution theory (IAST) via the previously cited single component adsorption data.

Keywords Adsorption · Co-adsorption · CO_2 · CO · CH_4 · H_2 · Gravimetry · Inverse gas chromatography · Zeolite · NaX · Synthesis gas · Isosteric heat

Abbreviations

S_{BET}	Specific surface area (m^2/g)
$V_{Dubinin}$	Micropore volume (cm^3/g)
q_s	Langmuir/Toth parameter 1 (mmol/g)
b	Langmuir/Toth parameter 2 (1/bar)
m	Toth parameter 3
m_{ads}	Adsorbed amount (mmol/g)
T	Temperature (K)
P	Pressure (kPa)
Y	Gas phase composition
X	Adsorbed phase composition
α	Selectivity
Ω	Reduced mass (g/g)
$V_{crucible}$	Volume of the crucible (cm^3)
$V_{adsorbent}$	Volume of the sample (cm^3)
$V_{adsorbed\ phase}$	Volume of the adsorbed phase (cm^3)

Y. Belmabkhout · G. Pirngruber (✉) · E. Jolimaitre · A. Methivier
Institut Français du Pétrole, Direction Catalyse et Séparation, Département Séparation, BP3, 69390 Vernaison, France
e-mail: gerhard.pirngruber@ifp.fr

1 Introduction

Synthesis gas (syngas), which is a mixture of H_2 and carbon oxides (CO and CO_2) and minor amounts of other gases, e.g. methane, nitrogen and hydrogen sulfide, is produced by thermal gasification of a various organic matter, including fossil fuels and biomass. Syngas is the main source for bulk H_2 production. In order to produce H_2 from synthesis gas, H_2 needs to be separated from the other components. High purity H_2, that meets hydrogen fuel cell specifications, is generally produced by Pressure Swing Adsorption (PSA) (Hufton et al. 1999; Yong et al. 2002). For the design and optimisation of PSA units, reliable adsorption data are required. Equilibrium adsorption measurements can be carried out using a wide range of techniques, which can be based on closed systems, such as gravimetric or volumetric methods (Belmabkhout et al. 2004; Keller and Staudt 2005), or open flow systems such as pulse or step experiments (Harlick and Tezel 2004; Delgado et al. 2006; Diaz et al. 2005), often subsumed under the term inverse gas chromatography (IGC).

Intensive investigations on adsorption thermodynamics and kinetics have been realised in order to find the appropriate conditions and adsorbents for further industrialisation. The experimental conditions of most investigations are limited to ambient temperature and low pressure (Barrer and Gibbons 1965; Walton et al. 2006). Very limited

work was devoted to high temperature/high pressure adsorption. Moreover, a complete set of adsorption data on CO_2, CO, CH_4 and H_2 is very scarce (Maurin et al. 2005; Akten et al. 2003; Harlick and Tezel 2004; Khelifa et al. 1999; Zhang et al. 1991; Kazansky et al. 1998; Wirawan and Creaser 2006; Pulin and Fomkin 2004).

In this work we assess the adsorption capacity and selectivity of syngas components in a wide range of temperature and pressure using static gravimetric and dynamic inverse gas chromatographic methods. For the purpose of illustration, we opted for a Na^+ form of faujasite X as an adsorbent and CO_2, CO, CH_4 and H_2 as adsorbates. Experimental loadings for the CO_2/CO binary adsorption were confronted to those extracted from macroscopic modelling by using IAST (Valenzuela and Myers 1989; Myers and Valenzuela 1965; Talu and Myers 1988).

2 Experimental

2.1 Adsorbates and adsorbents

CO (> 99.999 purity), CO_2 (> 99.995 purity), CH_4 (99.995 purity), and H_2 (99.999 purity) were provided by Air Liquide. NaX pellets were used as adsorbent. Based on a comparison of their micropore volume with that of NaX powder, the pellets contains 16 ± 1% binder. Table 1 shows the textural characteristics and elemental analysis of the sample.

2.2 Experimental methods

2.2.1 Low–high pressure gravimetry (LHPG)

The Rubotherm magnetic suspension balance (MSB) overcomes the disadvantages of other commercially available gravimetric instruments by separating the sensitive microbalance from the sample and the measuring atmosphere (Losch 1999; Dreisbach et al. 2003). This system is able to perform adsorption isotherm measurements while increasing the gas pressure from 0 to 15 MPa and for temperatures ranging from 303 to 473 K. Figure 1 shows a schematic representation of the Low–high pressure gravimetry (LHPG) apparatus. A clean (outgassed) adsorbent sample is exposed to a pure gas at constant temperature. The change in the weight of the adsorbent sample as well as pressure and temperature are measured when thermodynamic equilibrium is reached. This method allows the direct measurement of the reduced mass Ω. A correction for the buoyancy effect is required to determine the absolute adsorbed amount $m_{absolute}$ (Belmabkhout et al. 2004; Dreisbach et al. 2003) using (1). For this purpose the density of the gas is determined experimentally using a volume calibrated titanium-cylinder. By weighing this calibrated volume in the gas atmosphere, the local density of the gas is determined. Simultaneous sorption and gas phase density measurement as a function of pressure and temperature are, thus, possible.

$$\Omega = m_{absolute} - \rho_{gas}(V_{adsorbent} + V_{crucible} + V_{adsorbed\ phase}). \quad (1)$$

$V_{adsorbent}$ and $V_{crucible}$ are determined by the helium isotherm method, while $V_{adsorbed\ phase}$ can be extracted from the micropore volume (Keller and Staudt 2005). The effect of $V_{adsorbed\ phase}$ is negligible in the case of CO_2, CO, CH_4 in the whole range of the operational conditions studied.

The pressure is measured thanks to three kinds of pressure transmitters (two MKS Baratron PDR 2000 up to 100 Pa and 100 kPa respectively and a DRUCK DPI 280 up to 15 MPa). Prior to each adsorption experiment, about 1 to 2 g sample is outgassed using the in situ heating system under a constant residual pressure 10^{-6} kPa up to final temperature of 673 K. The temperature is held constant by using a circulating fluid thermostat.

2.2.2 Column breakthrough experiments

A scheme of the inverse gas chromatography setup can be seen on Fig. 2. The sample (5.6 g of hydrated NaX) was placed into a stainless steel column with an inner diameter of 1.0 cm and a length of 10 cm. The column was inserted in an oven and the sample was activated at 673 K for 3 hours under a helium flow-rate of 1 NL/h and then cooled to the adsorption temperature (323 or 373 K). The breakthrough experiments were performed by stepping from pure He to CO, CO_2 or mixtures thereof. The gas mixture leaving the column was analyzed by a mass spectrometer. All the experiments were performed at atmospheric pressure (the pressure drop in the column is negligible). The adsorbed amounts were calculated via a mass balance.

$$n_{i,ads} = F_{in} \cdot c_{i,in} \cdot t_{final} - \int_0^{t_{final}} F_{out} \cdot c_{i,out}(t) \cdot dt - (V_i + V_m) \cdot c_{i,in}, \quad (2)$$

Table 1 Elemental analysis and textural characteristics of NaX faujasite

Sample	% Si	% Al	% Na	Si/Al	S_{BET} m^2/g	$V_{Dubinin}$ cm^3/g	Loss on ignition % m/m
NaX	18.53	14.82	9.53	1.25	685	0.283	28.5

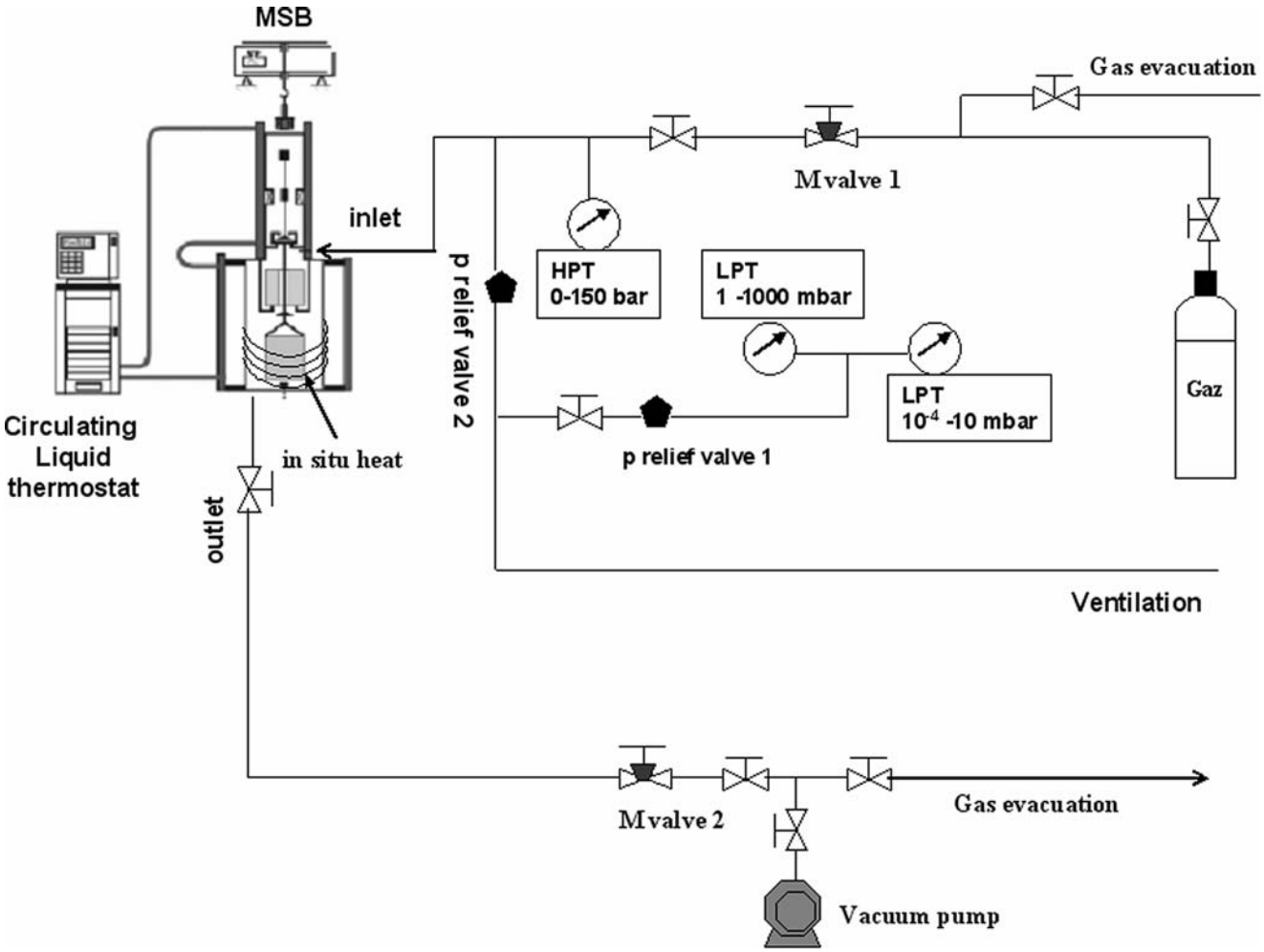

Fig. 1 Gravimetric experimental apparatus

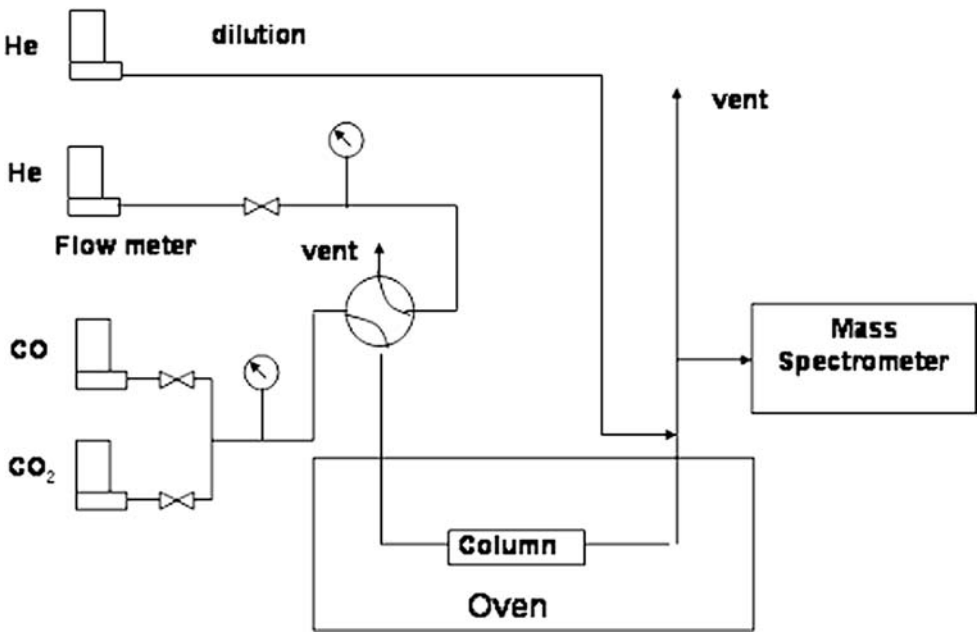

Fig. 2 Apparatus used for the column breakthrough experiments

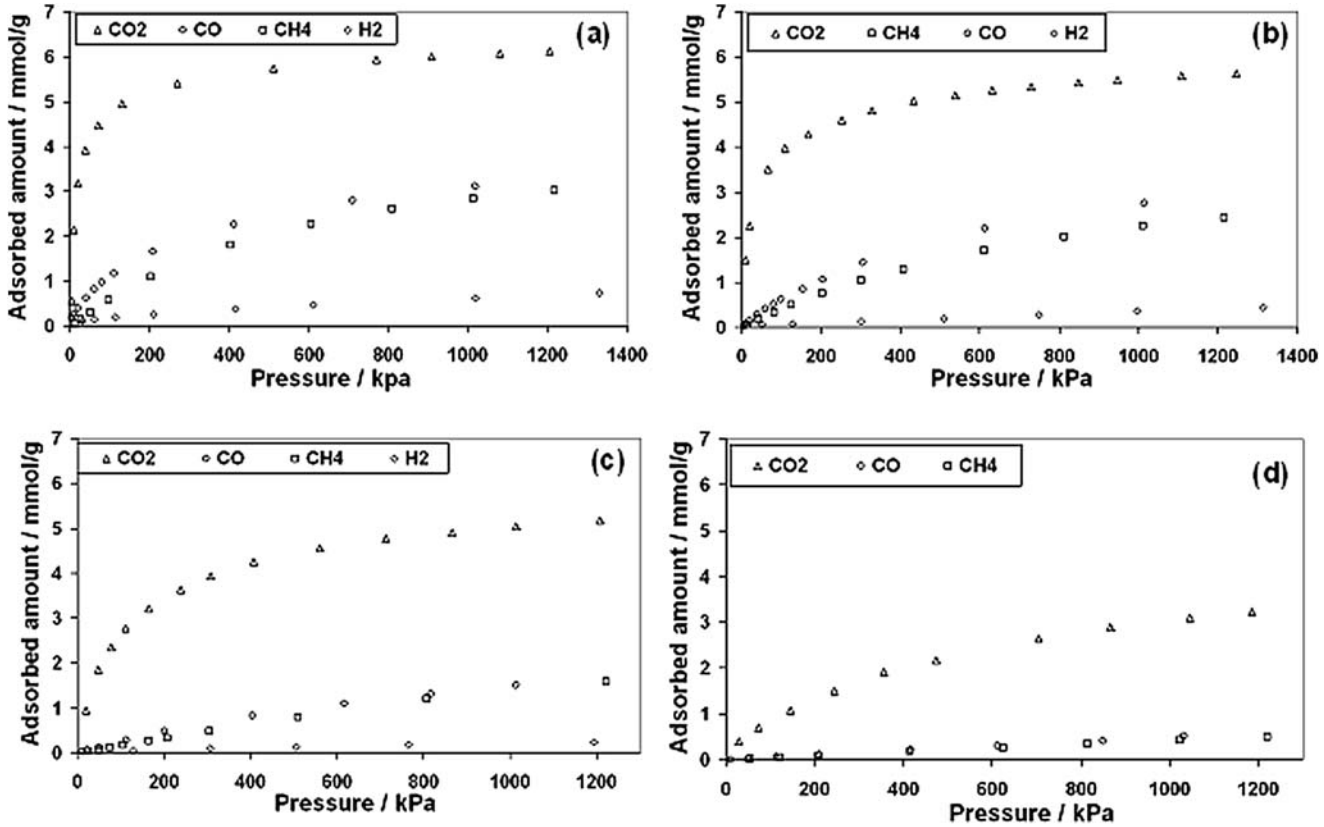

Fig. 3 Experimental adsorption isotherms of CO_2, CO, CH_4, and H_2 on NaX at 303 K (**a**), 323 K (**b**), 373 K (**c**) and 473 K (**d**)

F = total molar flow rate, c_i = molar fraction of component i, $V_i + V_m$: interstitial and macroporous/mesoporous column volumes.

The difficulty in column breakthrough experiments with highly concentrated gases that adsorb strongly is that the flow rate at the column outlet changes as a result of the adsorption process. $F_{out}(t)$ is not constant. It is therefore more convenient to measure directly the molar flow rate of the component i, i.e. $F_{i,out}(t) = F_{out}(t) * c_{i,out}(t)$, instead of its concentration. This is done by diluting the gas mixture leaving the column with a large excess of He (30 NL/h). The dilution serves two purposes: firstly, the concentrations are brought into a range where the response of the mass spectrometer is linear. Secondly, the measured concentration is directly proportional to $F_{i,out}(t)$ (see (3)):

$$c_{i,out}(t) = \frac{F_{i,out}(t)}{F_{i,out}(t) + F_{He}} \approx \frac{F_{i,out}(t)}{F_{He}}. \tag{3}$$

The mass fragments m/e = 44 and 28 were used to measure the concentrations of CO_2 and CO, respectively. Since CO_2 also has a mass fragment at m/e = 28, its contribution to the corresponding signal has to be subtracted to obtain the concentration of CO in experiments with CO_2/CO mixtures. The subtraction introduces an additional error in the determination of c_{CO}. The precision of the adsorbed amounts of CO is therefore lower than for CO_2.

3 Results and discussion

3.1 Single gas adsorption isotherms of CO_2, CO, CH_4 and H_2 on NaX

Figure 3 shows adsorption isotherms of CO_2, CO, CH_4 and H_2 in a wide range of pressures and temperatures (Tables 2–5 compile all the data). The adsorption always follows the order $CO_2 \gg CO > CH_4 \gg H_2$. Such a complete set of experimental data was not available before (Akten et al. 2003). CO_2 adsorbs most strongly on NaX because its quadrupole moment interacts with the electric field of NaX. Also CO has a weak quadrupole moment, whereas CH_4 interacts only through dispersion and polarization forces with extraframework cations and lattice oxygen of the zeolites. This explains why the adsorption of CO is slightly stronger than that of CH_4.

The isotherms can be satisfactorily fitted by the Langmuir (4) and Toth (5) models up to 300 kPa as shown

Table 2 Adsorption data on NaX pellets at 303 K

Pressure kPa	m_{ads} (CO_2) mmol/g	Pressure kPa	m_{ads} (CO) mmol/g	Pressure kPa	m_{ads} (CH_4) mmol/g	Pressure kPa	m_{ads} (H_2) mmol/g
5.02	0.555	5.94	0.182	12.15	0.049	27.11	0.067
10.81	2.145	10.78	0.256	26.68	0.145	53.30	0.080
21.39	3.171	20.41	0.389	50.81	0.298	125.1	0.109
38.73	3.920	40.45	0.619	97.84	0.570	321.3	0.186
69.02	4.465	61.2	0.813	202.9	1.090	613.5	0.279
132.1	4.946	80.4	0.967	403.1	1.803	1019.1	0.376
270.7	5.399	111.9	1.172	605.4	2.282	1523.7	0.499
511.4	5.743	209.0	1.649	809.7	2.611	2023.3	0.592
770.3	5.936	413.3	2.269	1013.0	2.846	3019.4	0.718
908.8	5.994	710.6	2.787	1216.3	3.023		
1080.7	6.070	1018.0	3.116				
1205.1	6.120						

Table 3 Adsorption data on NaX pellets at 323 K

Pressure kPa	m_{ads} (CO_2) mmol/g	Pressure kPa	m_{ads} (CO) mmol/g	Pressure kPa	m_{ads} (CH_4) mmol/g	Pressure kPa	m_{ads} (H_2) mmol/g
11.16	1.490	6.10	0.032	14.20	0.064	52.25	0.054
20.97	2.250	10.89	0.069	43.20	0.180	132.1	0.076
65.03	3.506	20.47	0.143	82.78	0.332	307.1	0.129
110.9	3.972	40.18	0.280	128.1	0.493	517.4	0.198
169.6	4.274	60.74	0.406	208.0	0.757	760.2	0.276
252.5	4.589	80.71	0.515	307.1	1.041	1012.0	0.357
329.4	4.803	100.2	0.613	408.2	1.293	1313.3	0.443
433.5	5.017	155.4	0.848	611.5	1.704	1813.9	0.578
538.7	5.147	205.0	1.057	812.7	2.011	2596.7	0.761
631.7	5.259	307.1	1.439	1011.0	2.246	2996.1	0.822
729.8	5.337	612.5	2.194	1216.3	2.440		
849.2	5.430	1014.0	2.746				

Table 4 Adsorption data on NaX pellets at 373 K

Pressure kPa	m_{ads} (CO_2) mmol/g	Pressure kPa	m_{ads} (CO) mmol/g	Pressure kPa	m_{ads} (CH_4) mmol/g	Pressure kPa	m_{ads} (H_2) mmol/g
20.90	0.945	11.25	0.032	25.59	0.040	132.1	0.067
48.21	1.856	21.37	0.058	51.07	0.082	312.2	0.104
78.55	2.346	50.46	0.130	76.19	0.127	513.4	0.134
111.9	2.769	112.9	0.280	104.8	0.174	776.3	0.177
165.5	3.213	201.7	0.488	164.5	0.270	1211.2	0.244
239.3	3.638	404.1	0.826	207.0	0.335	1826.1	0.327
309.1	3.932	617.6	1.105	306.1	0.482	2605.8	0.407
407.2	4.248	816.8	1.313	510.4	0.796	3062.9	0.431
560.9	4.562	1014.0	1.501	807.7	1.211		
712.6	4.770			1221.3	1.586		
865.3	4.909						
1013.0	5.043						
1207.1	5.176						

Table 5 Adsorption data on NaX pellets at 473 K

Pressure kPa	m_{ads} (CO_2) mmol/g	Pressure kPa	m_{ads} (CO) mmol/g	Pressure kPa	m_{ads} (CH_4) mmol/g
29.1	0.396	10.50	0.036	54.6	0.021
71.0	0.701	50.96	0.066	122.0	0.050
145.3	1.077	115.0	0.102	209.0	0.090
245.4	1.496	210.0	0.162	414.3	0.186
356.6	1.907	415.3	0.238	624.6	0.263
474.0	2.173	612.5	0.302	814.8	0.351
704.5	2.643	850.2	0.412	1022.1	0.433
866.3	2.882	1031.2	0.513	1219.3	0.507
1046.4	3.090				
1185.9	3.220				

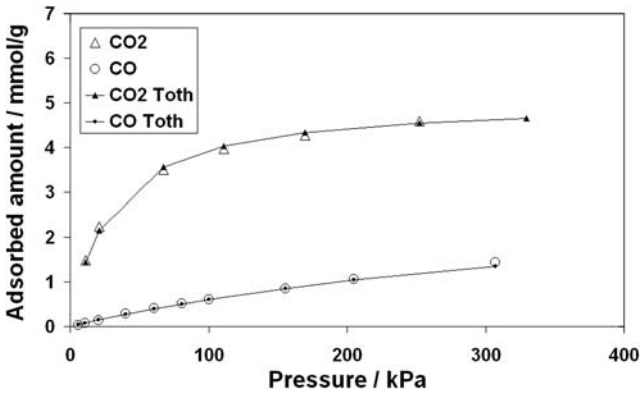

Fig. 4 Fit of experimental static CO_2 and CO measurements via Toth model at 323 K and up to 300 kPa

in Fig. 4:

$$q = q_s * \frac{bP}{(1+bP)} \tag{4}$$

$$q = q_s * \frac{bP}{(1+(bP)^m)^{1/m}}. \tag{5}$$

These fits will be used later for the prediction of binary adsorption via the IAST model. The key equations used in this theory are described, for example, in Myers and Valenzuela (1965).

Figure 5 shows a confrontation between static and dynamic single adsorption measurements at 323 and 373 K and 100 KPa. The agreement between the two techniques is excellent.

The isosteric heats of adsorption were calculated from the adsorption isotherms at the different temperatures and the results are shown in Fig. 6. The most important factor influencing the determination of the isosteric heat is the correct measurement of the sample temperature (in a magnetic suspension balance the thermocouple is never in touch with the sample). Generally, the estimated error of the isosteric heat varies between 20% to 5% depending on the nature of the gas, the temperature range and the loading range (the error is larger at low loadings).

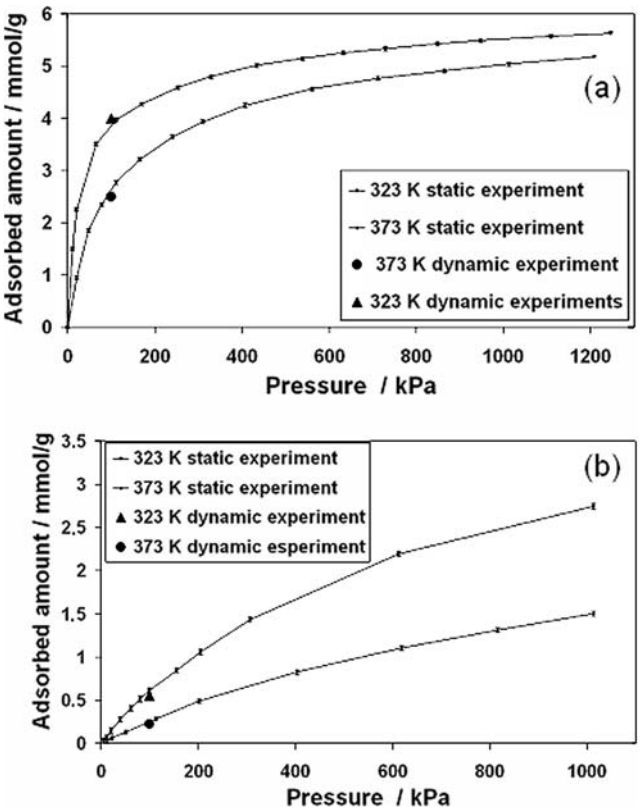

Fig. 5 Comparison between static and dynamics measurements (100 kPa) of CO_2 (**a**) and CO (**b**) adsorption at different temperatures

The isosteric heat of adsorption at 0.8 mmol/g for CO_2 in NaX (31.0 kJ mol^{-1}) is much higher than that of CO ($\approx$ 20 kJ mol^{-1}) and CH_4(18.8 kJ mol^{-1}), reflecting the stronger interaction between the CO_2 molecules and the Na^+ zeolite surface. These values are in good agreement with previous works (Pulin and Fomkin 2004; Maurin et al. 2005; Maurin et al. 2006). The weak H_2 adsorption does not allow

a reliable computation of the isosteric heat. Consequently the latter is not presented in Fig. 6.

At low loadings (< 1 mmol/g), a steep decrease of the CO_2 isosteric heat of adsorption can be noticed. A similar effect has been observed before (Maurin et al. 2005) and was attributed to the heterogeneity of the adsorption sites in NaX (site III′ and II) when the first molecules of CO_2 are adsorbed.

3.2 Multicomponent adsorption

We wanted to test whether the single component isotherms can be used to predict binary adsorption. The co-adsorption of CO and CO_2 was used as a test case. The binary adsorption data were predicted with the Ideal Adsorbed Solution Theory (IAST) and then confronted to experimental data obtained from column breakthrough experiments.

A typical binary mixture breakthrough curve—CO_2 (48.4%) /CO (51.6%) at 373 K and 100 kPa—is shown in Fig. 7.

The breakthrough of CO occured after only 170 s followed by CO_2 at about 1780 s. There is a roll-up of CO because initially adsorbed CO is replaced by incoming CO_2 until breakthrough of the latter occurs. The large difference in the breakthrough times of CO and CO_2 indicates that the CO_2/CO selectivity is very high.

Table 6 compiles the adsorption results from CO_2/CO binary breakthrough experiments with different initial gas compositions at 323 K and 373 K and 100 kPa. For all experimental conditions, the CO_2/CO selectivity is highly in favour of CO_2 and decreases with increasing temperature. Both effects were expected in view of the isosteric heats of CO and CO_2. At 323 K, the selectivity does not vary significantly with the gas phase composition. At 373 K, the selectivity seems to slightly increase in favour of CO_2 at smaller CO_2 partial pressures. However, one should keep in mind that high selectivity values are very sensitive to experimental errors.

The experimental results of the inverse gas chromatography were confronted to IAST simulations at 323 K and 373 K for a pressure of 100 kPa. The results obtained with Toth isotherms are presented in Figs. 8 and 9. The IAST predictions using Toth and Langmuir isotherms are very close.

The agreement between the adsorbed amounts obtained from IGC experiments and IAST is reasonable. Discrepancies are especially observed at low molar fractions of CO_2 in the mixture: in this case IAST systematically underestimates the amount of CO_2 adsorbed. We tentatively attribute this phenomenon to the non-ideality of the adsorbed phase. Non-ideal behaviour of the adsorbed phase of mixtures of CO_2 with apolar molecules (alkanes and alkenes) is well-known (Calleja et al. 1994; Siperstein and Myers 2001). In particular, mixtures of CO_2 and C_2H_6 behaved very similar to our CO_2/CO mixtures (Dunne et al. 1997).

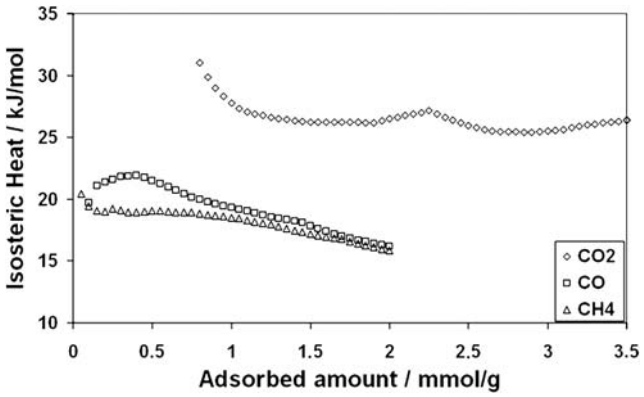

Fig. 6 Isosteric heat of adsorption of CO_2, CO, CH_4 on NaX

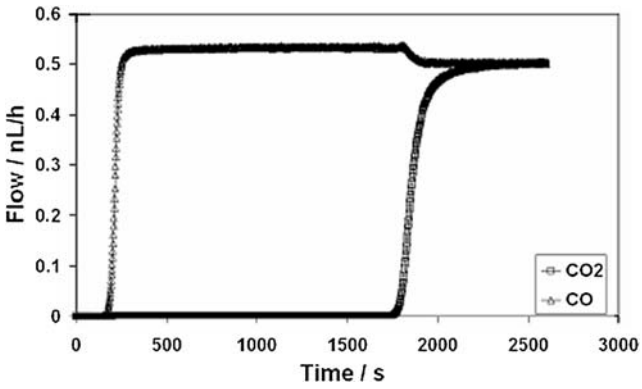

Fig. 7 Breakthrough curve for a CO_2 (48.4%)/CO (51.6%) mixture at 373 K and 100 kPa

Table 6 Results of the CO_2/CO breakthrough experiments

Temperature/K	Y(CO_2)	Y(CO)	m_{ads} (CO_2) mmol/g	m_{ads} (CO) mmol/g	α	α(IAST) Langmuir	Toth
323	0.174	0.826	2.51	0.183	62	28	31
	0.484	0.516	3.39	0.056	65	33	28
	0.804	0.196	3.85	0.014	65	37	26
373	0.174	0.826	1.22	0.114	51	24	24
	0.484	0.516	1.87	0.047	42	29	30
	0.804	0.196	2.35	0.017	34	34	43

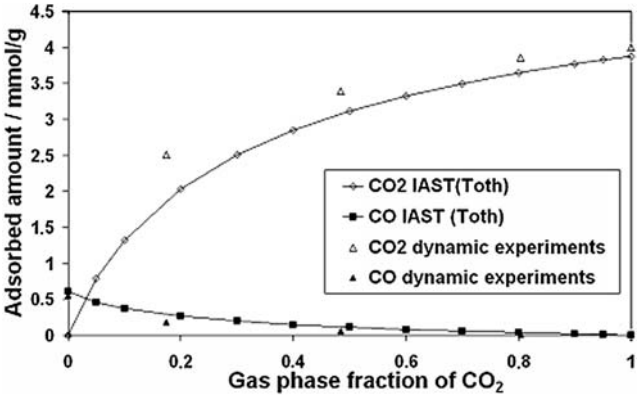

Fig. 8 Equilibrium curves: comparison with IAST at 323 K and 100 kPa

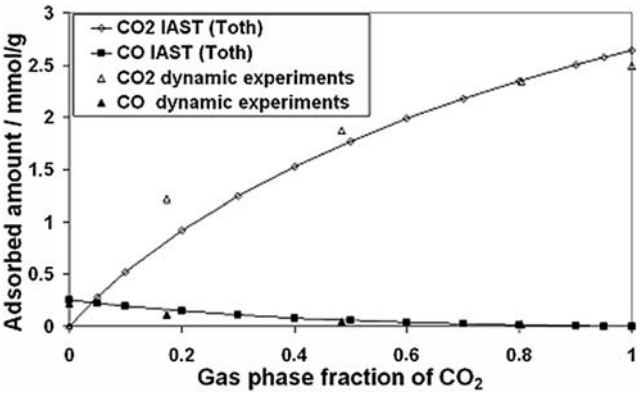

Fig. 9 Equilibrium curves: comparison with IAST at 373 K and 100 kPa

IAST also has difficulties to reproduce the experimentally observed selectivity values and their evolution as a function of composition. As above, this may be partly attributed to the non-ideal behaviour of the CO_2/CO mixtures. Moreover, it is important to note that the very high selectivity values are very sensitive to the corresponding errors of the adsorbed amount, for both IGC and IAST. The experimental decrease of selectivity with increasing temperature is qualitatively represented by the IAST model. This behaviour can be interesting for a high temperature PSA with the final aim to remove simultaneously CO_2, CO, CH_4 from syngas.

4 Conclusion

We have reported a comprehensive set of experimental data using both static and dynamic experiments which can be applied to a large variety of adsorption systems. A nice agreement between the two techniques for pure component equilibria was demonstrated. The accuracy of single gas data in a wide range of temperature using the gravimetric methods allows an accurate determination of isosteric heat of adsorption by varying temperature and pressure up to 1200 KPa and 473 K. The computed isosteric heats are in good agreement with microcalorimetric data at low loading and reflect the stronger interaction of NaX with CO_2 compared to CO and CH_4.

From the single adsorption isotherms, we have calculated the IAST selectivity of CO_2/CO in a wide range of temperatures and gas phase compositions and found a reasonable agreement to experimental binary breakthrough curves. The difference between IAST and experimental data is attributed to a non-ideality of the adsorbed CO_2-CO phase.

Acknowledgement This work was supported by EU funding via FP6-Marie Curie Research Training Network "INDENS" (MRTN-CT-2004-005503).

References

Akten, E.D., Siriwardane, R., Sholl, D.S.: Monte Carlo simulation of single- and binary-component adsorption of CO_2, N_2 and H_2 in zeolites Na-4A. Energy Fuels **17**, 977–983 (2003)

Barrer, R.M., Gibbons, R.M.: Zeolitic carbon dioxide: energetics and equilibria in relation to exchangeable cations in faujasite. J. Chem. Soc. Faraday Trans. 1 **61**, 948–961 (1965)

Belmabkhout, Y., Frère, M., De Weireld, G.: High-pressure adsorption measurements. A comparative study of the volumetric and gravimetric methods. Meas. Sci. Technol. **15**, 848 (2004)

Calleja, G., Jimenez, A., Pau, J., Dominguez, L., Pérez, P.: Multicomponent adsorption equilibrium of ethylene, propane, propylene and CO_2 on NaX zeolite. Sep. Purif. Technol. **8**, 247–255 (1994)

Delgado, J.A., Uguina, M.A., Sotelo, J.L., Ruiz, B., Gomez, J.M.: Fixed-bed adsorption of carbon dioxide/methane mixtures on silicalite pellets. Adsorption **12**, 5–18 (2006)

Diaz, E., Ordonez, S., Auroux, A.: Comparative study on the gas-phase adsorption of hexane over zeolites by calorimetry and inverse gas chromatography. J. Chromatogr. A **1095**, 131–137 (2005)

Dreisbach, F., Seif, R., Losch, H.W.: Adsorption equilibria of CO/H_2 with a magnetic suspension balance. Purely gravimetric measurements. J. Therm. Anal. Calorim. **71**, 73–82 (2003)

Dunne, J.A., Rao, M., Sircar, S., Gorte, R.J., Myers, A.L.: Calorimetric heat of adsorption and adsorption isotherms 3. Mixtures of CH_4 and C_2H_6 in silicalite and mixtures of CO_2 and C_2H_6 in NaX. Langmuir **13**, 4333–4341 (1997)

Harlick, P.J.E., Tezel, F.H.: An experimental adsorbent screening study for CO_2 removal from N_2. Microporous Mesoporous Mater. **76**, 71–79 (2004)

Hufton, J., Mayorga, S., Nataraj., S., Sircar, S.: Sorption-enhanced reaction process for the hydrogen production. Am. Inst. Chem. Eng. J. **45**, 248–256 (1999)

Kazansky, V.B., Borovkov, V.Y., Serich, A., Karge, H.G.: Low temperature hydrogen adsorption on sodium forms of faujasites: barometric measurement and drift spectra. Microporous Mesoporous. Mater. **22**, 251–259 (1998)

Keller, J., Staudt, R.: Gas Adsorption Equilibria. Experimental Methods and Adsorption Isotherms. Springer, New York (2005)

Khelifa, A., Derriche, Z., Bengueddach, A.: Sorption of carbon dioxide by zeolite X exchanged with Zn^{2+} and Cu^{2+}. Microporous Mesoporous Mater. **32**, 199–209 (1999)

Losch, H.W.: Renaissance of gravimetry in metrology under controlled environments—the magnetic suspension balance. In: Cooper, E. (ed.) Global Chemical Processing & Engineering Industry, p. 104. Mountain High Images (1999)

Maurin, G., Llewellyn, P.L., Bell, R.G.: Adsorption mechanism of carbon dioxide in faujasites: Grand Canonical Monte Carlo simulations and microcalorimetry measurements. J. Phys. Chem. B **109**, 16084–16091 (2005)

Maurin, G., Bourrelly, S., Llewellyn, P.L., Bell, R.G.: Simulation of the adsorption properties of CH_4 in faujasites up to high pressures. Microporous Mesoporous Mater. **89**, 96–102 (2006)

Myers, A.L., Valenzuela, D.P.: Thermodynamics of mixed-gas adsorption. AICHE J. **11**, 121–127 (1965)

Pulin, A.L., Fomkin, A.A.: Thermodynamics of CO_2 adsorption on Zeolite NaX in wide intervals of pressures and temperatures. Russ. Chem. Bull. **53**(8), 1630–1634 (2004)

Siperstein, F.R., Myers, A.L.: Mixed-gas adsorption. AICHE J. **47**, 1141–1159 (2001)

Talu, O., Myers, A.L.: Rigorous thermodynamic treatments of gas adsorption. AICHE J. **34**(11), 1887–1893 (1988)

Valenzuela, D.P., Myers, A.L.: Adsorption Equilibrium Data Handbook, pp. 208–216. Prentice Hall, Englewood Cliffs (1989)

Walton, K.S., Abney, M.B., LeVan, M.D.: CO_2 adsorption in Y and X zeolites modified by alkali metal cation exchange. Microporous Mesoporous Mater. **91**, 78–84 (2006)

Wirawan, S.K., Creaser, D.: Multicomponent $H_2/CO/CO_2$ adsorption ob BaZSM-5 zeolite. Sep. Purif. Technol. **52**, 224–231 (2006)

Yong, Z., Mata, V., Rodrigues, A.E.: Adsorption of carbon dioxide at high temperature—a review. Sep. Purif. Technol. **26**, 195–205 (2002)

Zhang, S.Y., Talu, O., Hayhurst, D.T.: High pressure adsorption of methane in NaX, MgX, CaX, SrX, and BaX. J. Phys. Chem. **95**, 1722–1726 (1991)